

- ¹²⁹, 664 (1963).
- ⁷Louis D. Roberts, Richard L. Becker, F. E. Obenshain, and J. O. Thomson, *Phys. Rev.* **137**, 895 (1965).
- ⁸H. Frauenfelder, *The Mössbauer Effect* (Benjamin, New York, 1962); O. C. Kistner and A. W. Sunyar, *Phys. Rev. Letters* **4**, 412 (1960).
- ⁹D. A. Shirley, *Rev. Mod. Phys.* **36**, 339 (1964); P. H. Barnett, R. W. Grant, M. Kaplan, and D. A. Shirley, *J. Chem. Phys.* **39**, 1035 (1963).
- ¹⁰R. M. Bozorth, *Ferromagnetism* (Van Nostrand, New York, 1951), p. 441.
- ¹¹Paul G. Huray, Louis D. Roberts, and J. O. Thomson, *Phys. Rev. B* **4**, 2147 (1971).
- ¹²A. Bohr and V. Weiskopf, *Phys. Rev.* **77**, 94 (1950).
- ¹³D. J. Erickson, Louis D. Roberts, J. W. Burton, and J. O. Thomson, *Phys. Rev. B* **3**, 2180 (1971).
- ¹⁴D. A. Shirley, M. Kaplan, and P. Axel, *Phys. Rev.* **123**, 816 (1961).
- ¹⁵David O. Patterson, J. O. Thomson, Paul G. Huray, and Louis D. Roberts, *Phys. Rev. B* **7**, 2440 (1970).
- ¹⁶R. L. Cohen, *Phys. Rev.* **171**, 343 (1968).
- ¹⁷H. Dahmen and S. Penselin, *Z. Physik* **200**, 456 (1967).
- ¹⁸S. Margulies and J. Ehrman, *Nucl. Instr. Method* **12**, 131 (1961).
- ¹⁹S. A. Ahern, M. J. C. Martin, and W. Sucksmith, *Proc. Roy. Soc. (London)* **248**, 145 (1958).
- ²⁰A. B. Balabanov and N. N. Delyagin, *Fiz. Tverd. Tela* **9**, 1899 (1967) [*Sov. Phys. Solid State* **9**, 1498 (1968)].
- ²¹I. K. Asayama, *J. Phys. Soc. Japan* **18**, 1727 (1963).
- ²²John C. Love, Felix E. Obenshain, and Gordon Czjek, *Phys. Rev. B* **3**, 2827 (1971).
- ²³J. Friedel, *Nuovo Cimento* **7**, 287 (1958).
- ²⁴B. Caroli and A. Blandin, *J. Phys. Chem. Solids* **27**, 503 (1966).
- ²⁵R. Ingals, H. G. Drickamer, and G. DePasquali, *Phys. Rev.* **155**, 165 (1967).
- ²⁶Thomas C. Tucker, Louis D. Roberts, C. W. Nestor, Jr., and Thomas A. Carlson, *Phys. Rev.* **178**, 998 (1969); Louis D. Roberts, David O. Patterson, J. O. Thomson, and P. R. Levey, *Phys. Rev.* **179**, 656 (1969).
- ²⁷E. C. Ellwood and K. Q. Bagley, *J. Inst. Metals* **80**, 617 (1952).
- ²⁸P. A. Flinn, B. L. Averback, and M. Cohen, *Acta Met.* **1**, 664 (1953).
- ²⁹Simon C. Moss, *Met. Soc. Conf.* **36**, 95 (1967).
- ³⁰B. R. Coles, *J. Inst. Metals* **84**, 346 (1956).

Energy Dependence of He⁺ and H⁺ Channeling in Si Overlaid with Au Films*

E. Lugujo[†] and J. W. Mayer

California Institute of Technology, Pasadena, California 91109

(Received 11 September 1972)

Channeling measurements by backscattering of He and H ions have been made on (111)- and (110)-oriented Si covered with evaporated layers of Au to investigate the dependence of minimum yield on both energy and film thickness. The energy range was 0.4–1.8 MeV and the film thickness range was 100–1100 Å. Minimum yields are calculated by applying the Meyer treatment of plural scattering and probability curves determined from (i) a step-function approximation to the angular yield profile and (ii) two different axial scans on uncovered Si, one of which is azimuthally averaged. The minimum yields calculated using the step-function approximation and azimuthally averaged probability curves are in good agreement with experimental results. This suggests that the step-function approximation, although less accurate than the azimuthally averaged procedure, is adequate for use with investigations of disorder in crystals by channeling-effect measurements.

I. INTRODUCTION

Many experimental and theoretical studies have established that the channeling of an energetic beam of particles in a single crystal occurs whenever the crystal axis or plane is aligned with the incident-beam direction. In the channeling process, the incident particles are steered by a series of gentle collisions with the lattice atoms of the rows or planes. In order for an energetic beam of particles to be steered by the lattice, the beam direction must be oriented within a certain critical angle ($\psi_{1/2}$) of the crystal axis or plane. The effect of channeling on particle trajectories in the

crystal is most strikingly observed in the significant reduction in processes requiring a close encounter with lattice atoms.¹⁻⁴

One of the parameters which has been measured in backscattering measurements is the minimum yield.² The minimum yield χ_0 is defined as the ratio of the number of backscattered particles when the incident beam is aligned with the crystal-symmetry direction of interest (aligned yield) to the number with the beam far from any high-symmetry direction of the crystal (random yield).

Channeling-effect measurements in crystals covered with amorphous layers have shown that the minimum yield of aligned spectra from the un-

derlying crystal increases with layer thickness.⁵⁻⁷ This increase in aligned yield is attributed to the scattering events in the amorphous layer which cause an increase in the transverse momentum of the particles incident on the underlying crystal.

A similar increase in aligned yield is observed in crystals containing lattice disorder such as ion-implanted Si⁸ or in epitaxially grown Si layers on spinel.⁹ In the determination of disorder by channeling effect measurements, one of the major problems in the analysis of aligned spectra is to separate the contribution from backscattering off displaced lattice atoms and that from dechanneling caused by the increase in transverse momentum due to forward scattering from the displaced atoms. In calculations of dechanneling, single-, plural-, and multiple-scattering treatments have been used. In most cases plural scattering seems to be appropriate.^{7,10,11} A simple method to test the analytical procedure is to superpose a known number of scattering centers in the form of an amorphous layer on the surface of a single crystal. Measurements of the aligned yield versus layer thickness or particle energy provides a good test of the assumptions underlying the analysis procedure.¹⁰

Recently, Andersen *et al.*¹² studied multiple scattering of ions through thin gold films. They found large deviations from theoretical predictions. Their results are in contrast with channeling measurements by backscattering of 1.8-MeV He ions that have been made on $\langle 111 \rangle$ - and $\langle 110 \rangle$ -oriented Si covered with evaporated layers of Au and Al.⁷ The minimum yield has been measured as a function of metal-film thickness and compared with the minimum yield predicted from Meyer's treatment¹³ of plural scattering using a step-function (square-well) approximation to the angular-yield profile. The step-function approximation assumes that particles scattered through angles greater than the critical angle are not channeled. It was found that experimental axial minimum-yield values agreed within 10% with step-function-approximation calculations.

It is difficult to make a direct comparison of the Andersen *et al.* measurements of half-widths of the multiple-scattering distributions with the channeling measurements of the number of particles scattered beyond the critical angle. It is possible, however, that use of the step-function approximation introduced systematic errors in the calculations of minimum yield to give fortuitous agreement with experimental values. One of the objectives of this present work has been to test the adequacy of the step-function approximation. This required measurements of angular-yield profiles on uncovered Si. Because of the isotropic-scattering distribution of the particles in the amorphous film, it was necessary to get azimuthally averaged an-

gular-yield profiles. Another objective was to measure the minimum yield as a function of particle energy. In this work, channeling measurements by backscattering of H and He ions ranging in energy from 0.4 to 1.8 MeV have been made on $\langle 111 \rangle$ - and $\langle 110 \rangle$ -oriented Si covered with evaporated layers of Au.

II. EXPERIMENT

Gold films from 100 to 1000 Å thick were vacuum deposited from a tungsten filament onto the $\langle 110 \rangle$ and $\langle 111 \rangle$ surfaces of silicon single crystals at room temperature. Each Si sample was masked so that a small area of it remained uncovered at the end of evaporation of the gold film. The evaporations were made in a vacuum of about 5×10^{-7} Torr.

Channeling measurements were made using the backscattering technique. Low-energy (400-keV) and high-energy (1.0 to 1.8-MeV) channeling experiments were done using accelerators at North American Rockwell Science Center and Caltech, respectively. Collimated beams (~ 2 -mm beam diameter) of protons and helium ions were accelerated onto samples mounted on a two-axis goniometer in a scattering chamber. The samples could be rotated and tilted with respect to the incident beam. The scattering chamber was evacuated to less than 10^{-5} Torr and secondary electrons were suppressed. The particles backscattered from the target through a laboratory angle of 168° were detected by a 25-mm² solid-state silicon-surface-barrier detector placed 10 cm away from the target. The energy spectrum of these particles was obtained using standard electronics and a 400-channel pulse-height analyzer. The energy resolution of the system was ≤ 15 keV for 1.8-MeV He ions.

Energy spectra of backscattered particles from an uncovered part of the Si sample were obtained using H and He ions (i) when a low-index direction ($\langle 111 \rangle$ or $\langle 110 \rangle$) was well aligned with the incident-beam direction (aligned spectrum) and (ii) when the beam was incident in a random direction (random spectrum). The random spectra on uncovered portions of the sample were obtained by tilting the sample off a major axial direction by an angle greater than ten times the critical angle for channeling at a given incident energy and continuously rotating the crystal about the beam direction. The aligned and random spectra on covered portions of Si samples were obtained by first obtaining the goniometer alignment settings by measuring the yield with the beam incident on the uncovered portion of the sample and then translating the beam to the covered portion. From experimental geometry, translation of the beam causes a change of 0.3×10^{-3} rad in the angle of incidence. Measurements on the uncovered sample showed that translation of the beam had no effect on the aligned components

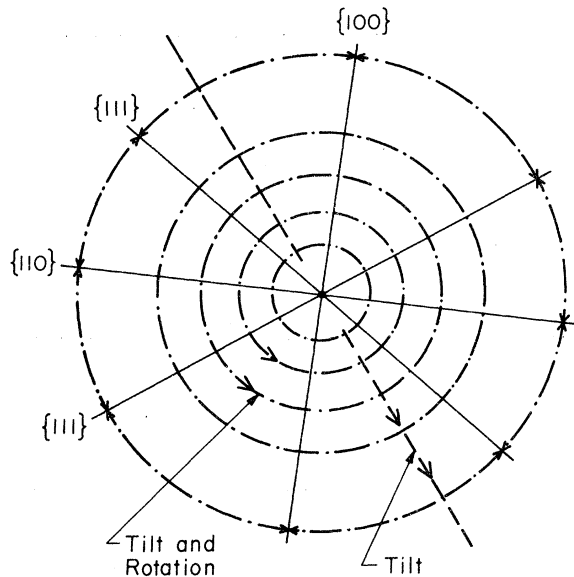


FIG. 1. Dashed line shows the tilt direction along which the normal axial angular-yield profile is obtained. The dash-dot lines represent the rotation direction along which an azimuthally averaged probability curve is obtained for various tilt angles. Solid lines are the Si crystallographic planes.

of the spectra.⁷

Backscattering techniques were used in measuring the thickness, uniformity, and amorphous nature of the Au films. The number of Au atoms per cm² was determined by integrating the counts under the Au spectrum. Representative values of the stopping cross section of Au for He⁺ particles at 0.5, 1.0, 1.5, and 1.8 MeV are 112.0, 128.0, 122.0, and 116.0 × 10⁻⁵ eV cm², respectively. These values were obtained from a fourth-degree-polynomial fit to the stopping cross-section data of Gobeli,¹⁴ Comfort *et al.*,¹⁵ and Porat and Ramavartan.¹⁶ For simplicity here, the Au-film thickness is given in angstroms and the conversion factor for Au is 5.9 × 10¹⁷ Au atoms/cm² being equivalent to 1000 Å. The energy loss per angstrom for in and out trajectories of backscattered particles is calculated from the energy-loss parameter S given by¹⁷

$$S \cong K^2 \frac{dE}{dx} \Big|_{E_{in}} + \frac{1}{|\cos\theta_L|} \frac{dE}{dx} \Big|_{K^2 E_{in}}$$

Representative values for S are 140.0, 134.2, and 132.0 eV/Å at 1.5-, 1.8-, and 2.0-MeV He⁺, respectively. The uniformity of the thicker Au films was deduced from the absence of any anomalous features in the trailing edges of the Au spectra. However, for Au films below 150 Å thick, the spectra revealed that about 10% of the Si substrate was uncovered. When the beam was aligned with the <111> or <110> axial directions, no change was ob-

tained in the Au signal from that obtained with a random incidence. So if these films are polycrystalline, the crystallites are either very small or their orientation is sufficiently random to allow the treatment of these Au films as amorphous structures for channeling experiments.⁷

Axial angular-yield profiles were determined on uncovered Si crystals oriented along <110> and <111> axial directions for 1.8-MeV He⁺ and 0.4-MeV H⁺. Two different methods were applied in obtaining these axial-yield profiles. The first method followed the usual procedure of performing an axial scan^{2,7} where the beam is first aligned with either <110> or <111> axial directions and then the normalized yield of particles backscattered from just below the surface of Si is obtained as a function of tilt angle. The direction of the tilt is indicated by the dashed line in Fig. 1 which shows the measured coordinates of the planes and <110> axes. The normalization of the yield was made to that of the random yield. The accuracy of the scan was checked by comparing both the minimum yield and the critical-angle value with those obtained in previous measurements at 0.4-MeV H⁺ and 1.8-MeV He⁺.⁴

In the second method, the sample is rotated at each tilt position thus giving an azimuthally averaged yield profile. In this method the beam was first aligned with the <110> axial direction of an uncovered Si crystal. Then the <110> axial direction was made collinear with the goniometer axis of rotation and the incident beam direction using the alignment stage mounted on the goniometer. This stage has two axes of rotation with respect to the incident-beam direction. It could be tilted so that the axial direction of the crystal resting on it could be brought in line with the axis of rotation of the goniometer. The normalized yield of the particles backscattered from just below the surface of Si was obtained as a function of tilt angle by continuously rotating the Si crystal about the beam direction (see Fig. 1). As before, the normalization of the backscattered yield was made to that of the random component of the dechanneled beam.

The scans obtained by those two above procedures coincide for both zero- and large-tilt angles. However, for tilt angles in between the critical angle $\psi_{1/2}$ and $\approx 3\psi_{1/2}$, the angular-yield profile obtained in the second method is lower than that in the first procedure. This lower yield is due to the influence of planar channels during azimuthal averaging by rotation of the sample around the crystal axes.

III. CALCULATION PROCEDURE

The presence of an amorphous layer on a silicon crystal results in an increase in the aligned yield of energy spectra of backscattered particles. The increase in the aligned yield can be calculated

from the scattering experienced by particles traversing the amorphous layer, the deflections produced by the crystal potential, and the channeling parameters such as the critical angle within the crystal. Since scattering in the layer introduces an angular dispersion into the initially well-collimated beam, the fraction of the beam that does satisfy the channeling condition decreases. Hence the ratio (minimum yield χ_0) of the aligned and random yield near the surface of the crystal increases (see Fig. 2).

Recently, channeling-effect measurements have been performed on Si overlaid with amorphous layers to investigate the dependence of minimum-yield values on amorphous-layer thickness at 1.8-MeV He⁺.⁷ The experimental minimum-yield values were compared with those predicted from knowledge of scattered-particle distribution in the amorphous layer and the channeling parameters in a Si single crystal. The scattered-particle distribution in the amorphous layer was based on two treatments of plural scattering. The first treatment of plural scattering is that of Keil *et al.*¹⁸ This utilizes the Molière¹⁹ cross section which is smaller than the Thomas-Fermi cross section and gives a strong forward-peaked distribution of the particles. The second treatment by Meyer¹³ uses the Thomas-Fermi cross section and the distribution of particles is not as peaked as that of Keil *et al.* in the plural regime. However, both treatments merge with each other for a large number of scattering centers. In these two treatments of plural scattering, film thicknesses are specified by a parameter m which gives the mean value of the number of collisions of the particles with the target atoms for a cross section of $\pi(a_{TF})^2$, a_{TF} being the Thomas-Fermi screening parameter. Representative values for m are 2.5 and 2.2 equivalent to 1100 Å of Au for He⁺ and H⁺, respectively.

We used several methods to calculate the aligned yield from a single crystal covered with an amorphous layer. One method for calculating the minimum yield utilizes both the experimental angular-yield profile obtained near the surface of the uncovered crystal and the calculated differential-scattering distribution of the particles in the film. In this method the yield is obtained by convolution of the initial scattering distribution in the amorphous layer with the experimental normalized angular yield profile. In this case we take the yield profile as a weighting function. This weighting function is first multiplied by the scattering distribution and then integrated over all angles to give the minimum yield. In this work two different procedures have been applied in obtaining axial-angular-yield profiles (one by tilting and the other by tilting and rotating the crystal to obtain an azimuthal average).

Another procedure used in determining the mini-

um yield involves a step-function approximation to the angular-yield profile. In this case the normalized yield is zero for angles less than $\psi_{1/2}$ (the critical angle for channeling) and unity for angles greater than $\psi_{1/2}$. We will refer to this probability curve as the "step-function approximation" to distinguish it from the general "convolution" procedure discussed in the first methods.

IV. RESULTS AND DISCUSSION

Figure 2(a) shows two typical energy spectra of backscattered particles from the uncovered part of the Si sample obtained using 1.8-MeV He ions (i) when the $\langle 111 \rangle$ axial direction is well aligned with the incident-beam direction (aligned spectrum) and (ii) when the beam is incident in a random direction (random spectrum). The random spectrum on an uncovered part of the Si crystal was obtained by first tilting the sample several degrees off a major axial direction and then continuously rotating the crystal about the beam direction. Figure 2(b) shows the spectra of the Si sample covered with 220 and 590 Å of Au. These spectra were obtained first by getting the aligned and random yield on an uncovered portion of the sample and then translating the incident 1.8-MeV He⁺ beam to a covered portion. The presence of the Au film on the Si substrate causes a shift in the Si edge to lower energy because of the energy losses of the particles as they traverse the film. The aligned yield increases with the film thickness. The uniform nature of the

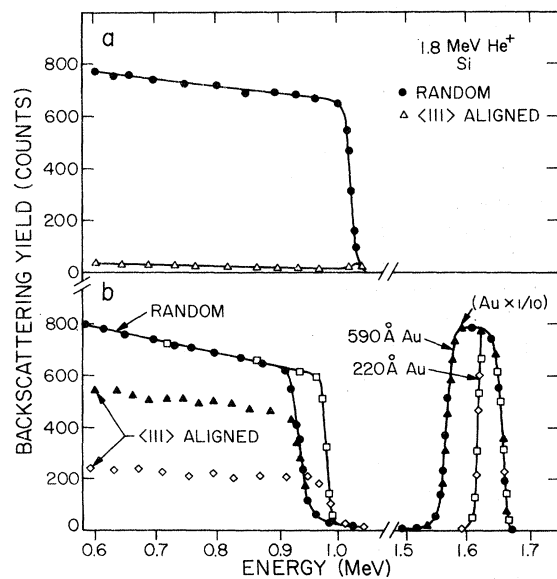


FIG. 2. Energy spectra for 1.8-MeV He⁺ backscattered (a) from an uncovered Si crystal for random (●) and $\langle 111 \rangle$ -aligned direction (Δ); (b) from a Si crystal covered with 590 and 220 Å of Au for random (● and □) and $\langle 111 \rangle$ -aligned directions (▲ and ◇), respectively.

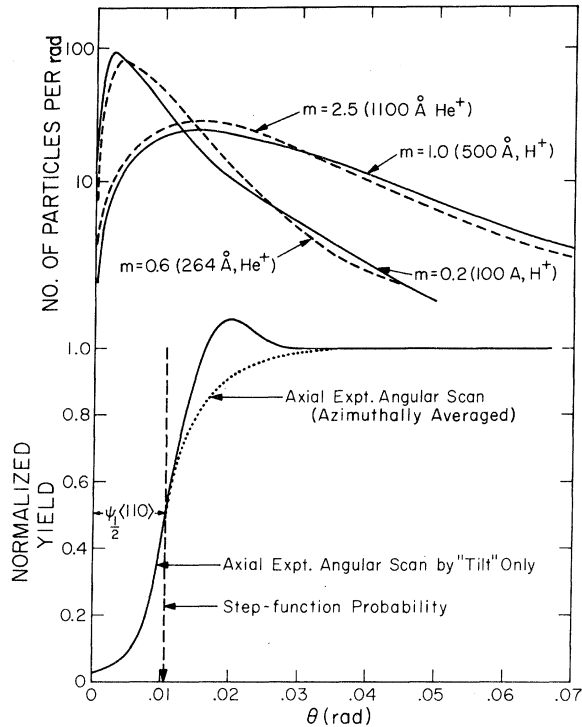


FIG. 3. Upper: number of particles scattered at angle θ from the initial direction for 0.4-MeV H^+ and 1.8-MeV He^+ after traversing a reduced thickness $m=0.2$ (100- \AA Au, H^+), $m=1.0$ (500- \AA Au, H^+) (solid lines), and $m=0.6$ (264- \AA Au, He^+), $m=2.5$ (1100- \AA Au, He^+) (dashed lines) according to Meyer's theory. Lower: experimental axial scan obtained by "tilt" only (solid line) and azimuthally averaged experimental axial scan obtained by "tilt and rotation" (dotted line) for 1.8-MeV He^+ incident along $\langle 110 \rangle$ Si axis. Step-function approximation is shown as a vertical dashed line.

film is deduced from the smooth pattern of the Au signal and the absence of trailing edges at around 1.5 and 1.6 MeV of the Au spectra. The "amorphous" nature of the film is indicated by the fact that the aligned and random yields from the Au film coincide.

Figure 3 shows the calculated differential-scattering distributions $2\pi\theta f(\theta)$ which give the number of particles scattered by an amorphous layer at an angle θ from the initial direction for He^+ and H^+ ions. These differential distributions are obtained from the angular distribution tabulated by Meyer for $m=0.6$ (264- \AA Au, 1.8-MeV He^+), $m=2.5$ (1100- \AA Au, 1.8-MeV He^+), $m=0.2$ (100- \AA Au, 0.4-MeV H^+), and $m=1.0$ (500- \AA Au, 0.4-MeV H^+). The parameter m is the reduced thickness described in the Appendix. In the lower part of Fig. 3 are two experimental axial angular-yield profiles on uncovered $\langle 110 \rangle$ -oriented Si at 1.8-MeV He^+ . The yield profile (solid line) was obtained from experimental energy spectra recorded for

He ions at different incident tilt angles. The yield profile (dotted line) made on the Si $\langle 110 \rangle$ axial direction at 1.8-MeV He^+ was obtained by rotation of the crystal about the beam direction as a function of the tilt angle for a fixed charge. This yield profile without shoulders is the azimuthally averaged probability curve. Also shown in the vertical dashed curve is the step-function approximation for 1.8-MeV He^+ on the Si $\langle 110 \rangle$ axial direction.

Figure 4 shows the experimental minimum-yield values as solid triangles for the Si $\langle 110 \rangle$ axial direction at 1.8-MeV He^+ and open triangles for the Si $\langle 111 \rangle$ axial direction at 0.4-MeV H^+ . The minimum-yield values obtained by convolution of the differential distributions of He and H ions in the film and the angular-yield profiles obtained by tilt only for 1.8-MeV He^+ and 0.4-MeV H^+ on uncovered Si are shown in solid curves. For He ions, the convoluted minimum-yield values are about 5% higher than the experimental values for low and high m values. However, for intermediate m values, the minimum-yield values lie about 10% higher than the experimental ones. In the case of 0.4-MeV H^+ the convoluted yield values are higher than the experimental values by about 7% for the entire range of gold thicknesses.

On the other hand, when the azimuthally averaged angular-yield profile (shown in the dotted line in Fig. 3) is convoluted with the calculated differential-scattering distribution of He ions, the resultant minimum-yield values (shown by the dotted curves in Fig. 4) agree fairly well with the experimental data for the entire film thickness. This suggests that the most accurate angular-yield profile to use in convolution procedure is the curve obtained by tilting and rotation.

Shown in the dashed curves in Fig. 4 are the minimum-yield values obtained by applying the step-function approximation to Meyer's theory of plural scattering. The minimum yield is given by the integral of the differential-scattering distribution for angles greater than the critical angle for channeling $\psi_{1/2}$. These minimum-yield values are in good agreement with experiment for nearly all m values for both He and H ions. In fact, these values nearly coincide with those obtained by convolution using an azimuthally averaged angular-yield profile for gold thicknesses up to about 700 \AA . However, there is a systematic difference of about 3% for thicker films. A method of obtaining minimum-yield values from Meyer's treatment of plural scattering is described in the Appendix.

Also shown in the insert of Fig. 4 is a comparison of experimental Al minimum-yield values (from Ref. 7) with those obtained by applying the Meyer treatment of plural scattering and normalized yield curves determined from (a) the step-function approximation, (b) the axial angular scan

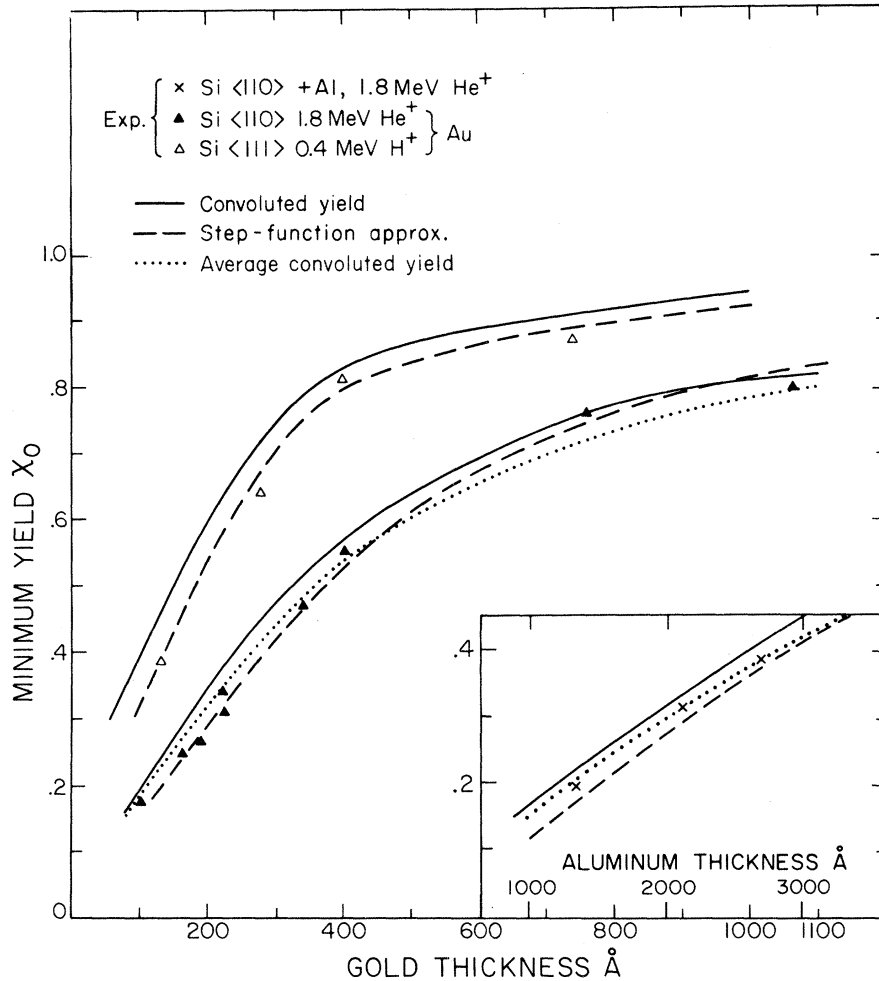


FIG. 4. Minimum yield χ_0 at the Si surface for 0.4-MeV H⁺ and 1.8-MeV He⁺ incident, respectively, along the <111> (Δ) and <110> (\blacktriangle) axes of Si covered with different thicknesses of Au. The lines show the calculated values using the Meyer distribution and (i) the step-function approximation (dashed line), (ii) the normal axial angular-yield profile (solid line), and (iii) the azimuthally averaged angular-yield profile (dotted line). Shown in the insert is the minimum yield χ_0 at the Si surface for 1.8-MeV He⁺ incident along the <110> axis (\times) of Si covered with different thicknesses of Al. The curves carry the same meaning as in the case of Au above.

obtained by tilt only, and (c) the azimuthally averaged angular-yield profile. Calculated minimum-yield values from the azimuthally averaged profile are in excellent agreement with experimental values. Also, there is adequate agreement with calculations based on the step-function approximation.

Figures 5(a) and 5(b) show the minimum-yield dependence on He⁺ and H⁺ energy and gold thickness, respectively. The solid curves are obtained by application of the step-function approximation to the scattering distribution in the Meyer theory. The experimental minimum-yield values (χ_0) are in accord with the theoretical prediction except for low thickness. For 130-Å Au the experimental values for He⁺ are slightly above the theoretical curve and below the theoretical curve for H⁺. In any case, the difference between theory and experiment is within 5%.

Figure 6 shows minimum-yield values for 400-keV He and H ions for <111>-oriented Si versus the reduced thickness of Au. The theoretical curves were obtained by application of the step-function approxi-

mation to both the Meyer and Keil treatments of plural scattering. The upper solid and dashed lines in Fig. 6 correspond to minimum yields calculated from Meyer distributions for 400-keV He and H ions, respectively. The lower set of curves correspond to those using Keil distributions at the same energy. It is very evident that the experimental minimum-yield values follow those calculated from the Meyer distributions very closely.

V. SUMMARY

Channeling-effect measurements have been used in investigating the minimum yield χ_0 at different He⁺ and H⁺ energies for various Au film thicknesses deposited on Si single crystals. These measurements indicate that the minimum yield increases with film thickness. In order to compare the experimental and predicted minimum-yield values, knowledge of the scattering in the film as well as the channeling behavior in the Si single crystal is necessary.

The scattering distribution in the film is based

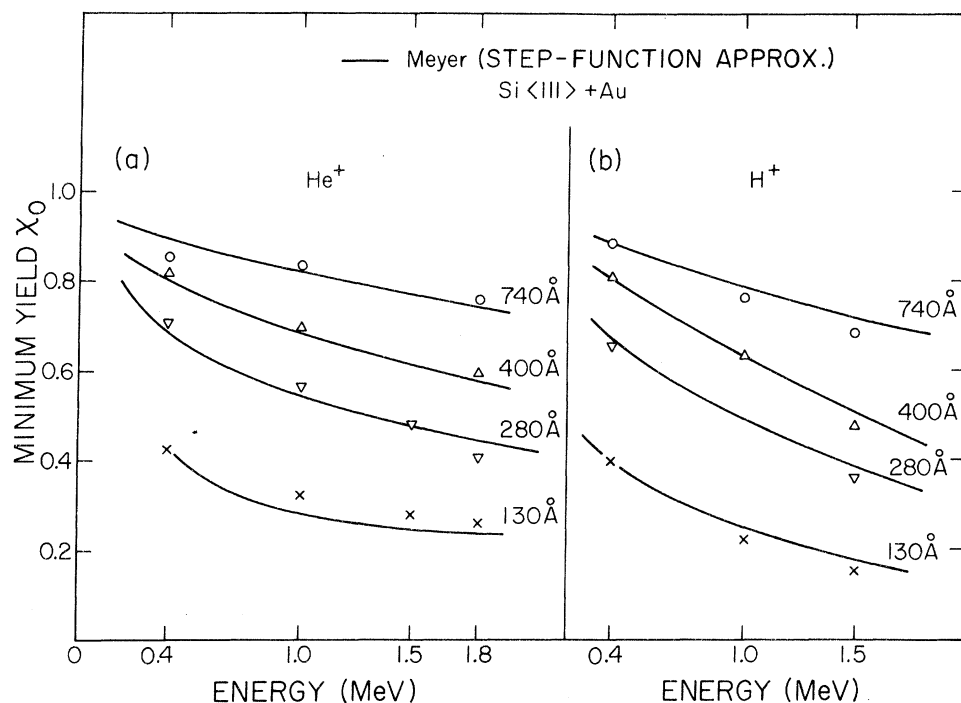


FIG. 5. Minimum yield χ_0 at the silicon surface as a function of (a) He^+ energy and (b) H^+ energy incident along the $\langle 111 \rangle$ axis of Si covered with different thicknesses of Au. The lines are calculated by using Meyer distribution and step-function approximation.

on the Meyer treatment of plural scattering. The channeling behavior in the Si single crystal was obtained by performing two different experimental axial scans on uncovered Si. Each of these scans is treated as a normalized-yield function. The first method which involves only tilting is experimentally easier to obtain but leads to higher (by about 10%) minimum-yield values than the experimental curves. These higher values are a consequence of the fact that the angular-yield profile was obtained by tilting the sample in a manner that avoided planar channels. However, some fraction of the particles scattered in the amorphous film will be incident on the crystal with directions aligned with planar channels. Consequently, this conventional method of obtaining angular-yield profiles by tilting is not an adequate procedure for obtaining normalized-yield functions.

The second method of obtaining an angular-yield profile involves tilt and rotation and hence provides an azimuthal average which includes the effect of planar channels. The angular-yield profiles obtained in this fashion give a more representative average normalized yield. The calculated minimum-yield values obtained from these average angular-yield functions and Meyer differential-scattering distributions are in good agreement with experimental values for Si covered with Au and Al. At present we cannot account for the differences between our results and those of Andersen *et al.* who found significant deviations from Meyer's prediction of reduced half-widths.

However, in the case of our channeling measurements, we are only sensitive to scattering angles greater than the critical angle.

The azimuthally averaged yield functions are difficult to obtain experimentally as the procedure requires that the crystallographic axis of the sample be aligned with the axis of rotation of the goniometer to better than one-quarter of the critical angle. A simpler analytical procedure is to use the step-function approximation. The assumption that the minimum yield is determined by the number of particles scattered beyond the critical angle (step-function approximation) has been tested for various Au-film thicknesses deposited on $\langle 111 \rangle$ and $\langle 110 \rangle$ Si-oriented crystals using 0.4–1.8-MeV He and H ions. The results are in agreement with experimental values. This suggests that the step-function approximation is adequate for use in investigations of disorder in crystals by channeling-effect measurements. As a prelude to disorder analysis, we have established universal curves from which minimum-yield values can be obtained for various disordered depths.

ACKNOWLEDGMENTS

The authors wish to acknowledge the contribution of E. Rimini who provided a stimulus for this investigation. They are also grateful to F. H. Eisen who made channeling measurements at low energy possible at North American Rockwell Science Center. Discussions with him and M.-A. Nicolet were greatly appreciated. W. K. Chu has

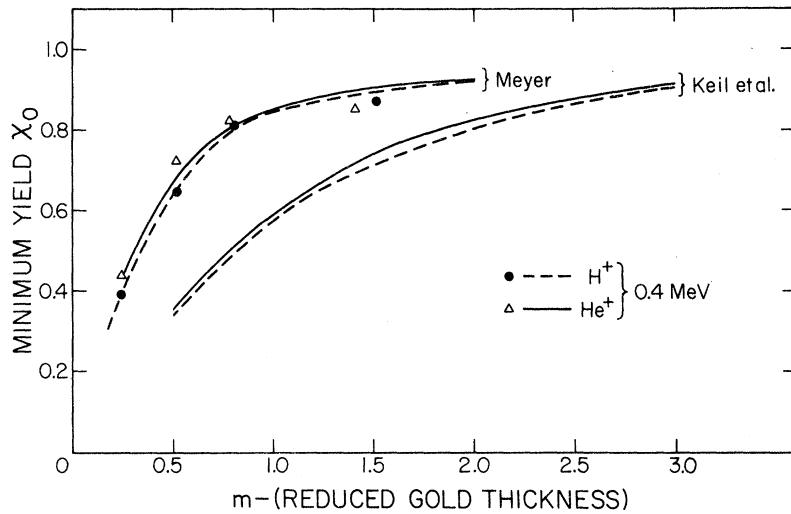


FIG. 6. Minimum yield χ_0 at the Si surface for 0.4-MeV H⁺ (●) and 0.4-MeV He⁺ (Δ) incident along the $\langle 111 \rangle$ axis of Si covered with various m values (the reduced gold thickness). The solid and dashed lines are calculated by using step-function approximation and the Meyer (upper) and Keil *et al.* (lower) treatment of plural scattering.

been of invaluable help in measuring the azimuthally averaged angular-yield profiles. We thank J. U. Andersen and K. Björkqvist for their comments on the first draft.

APPENDIX

This appendix gives a method of calculating the minimum yield from a crystal overlaid with an amorphous crystal film by applying the step-function approximation and the distribution of the scattered particles given by Meyer.¹³ Figure 7 shows

a plot of the minimum yield $P(\tilde{\theta}_c)$ as a function of the reduced critical angle $\tilde{\theta}_c$ for various reduced film thicknesses m [see Eq. (9)]. The reduced critical angle is given by $\tilde{\theta}_c = Y\psi_{1/2}$, where $\psi_{1/2}$ is the critical angle for channeling and Y is given in Eq. (15). For example, for 1.8-MeV He⁺ incident on 440 Å of Au on $\langle 110 \rangle$ -oriented Si, $m = 1.0$ and $Y = 41.6$. The critical angle $\psi_{1/2} = 0.01$ rad and hence $\tilde{\theta}_c = 0.42$ rad. The minimum-yield value taken from Fig. 7 is $P(0.42) \approx 0.57$. For 1550 Å of Al, $m = 10$ and $Y = 420$, the minimum-yield value

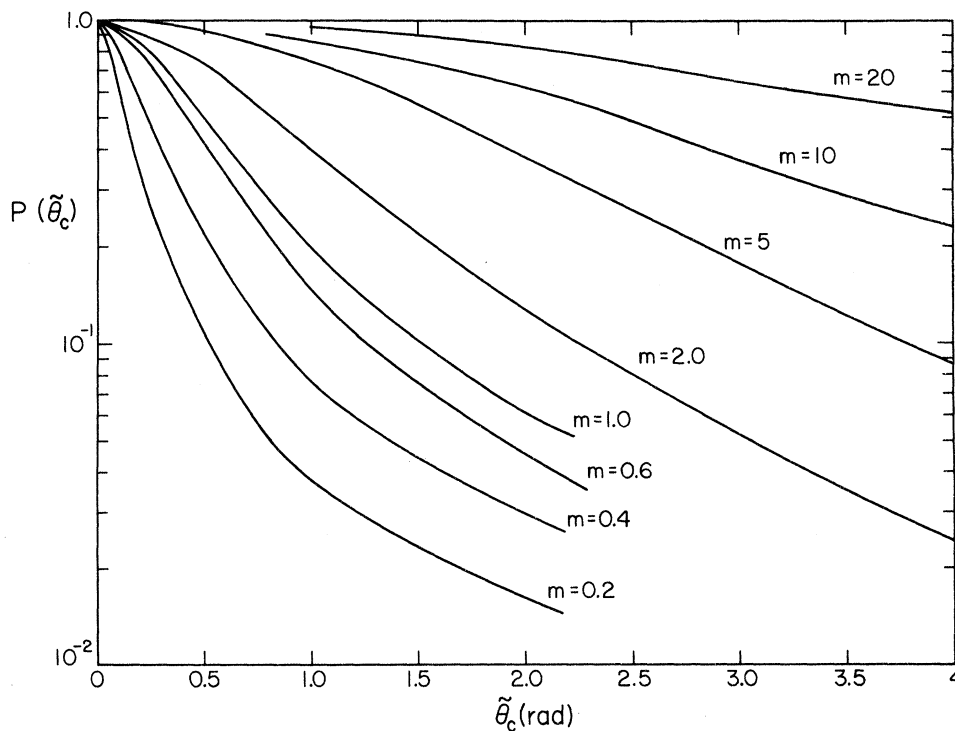


FIG. 7. Solid lines represent the normalized integrated differential distribution using the Meyer treatment vs reduced critical angle for various m values (the reduced thickness of amorphous layers). Minimum yield χ_0 is obtained from these curves by $\chi_0 = P(\tilde{\theta}_c)$.

is $P(4.2) \cong 0.20$. The details of the calculation are given below.

Meyer, using a scattering cross section derived from classical mechanics, presents calculations on small-angle multiple scattering of low-energy heavy particles in solid layers. He gives the following angular distribution of particles scattered in thin layers:

$$F(m, \tilde{\theta}) = \frac{1}{2\pi} \frac{\epsilon^2}{4} \left(\frac{m_1 + m_2}{m_2} \right)^2 \times [f_1(m, \tilde{\theta}) - \pi a^2 N^{2/3} f_2(m, \tilde{\theta})], \quad (\text{A1})$$

where

$$f_1(m, \tilde{\theta}) = \int_0^\infty e^{-m\Delta(z)} J_0(\theta z) z dz, \quad (\text{A2})$$

$$f_2(m, \tilde{\theta}) = \frac{1}{2} m \int_0^\infty e^{-m\Delta(z)} J_0(\tilde{\theta} z) \Delta^2(z) z dz, \quad (\text{A3})$$

and

$$\Delta(z) = \frac{1}{4} \int_0^\infty f(y) \{1 - J_0[z(\frac{1}{2}y)]\} dy. \quad (\text{A4})$$

J_0 is the zeroth-order Bessel function of the first kind and f is a scaling function given for different potentials in the work of Lindhard, Nielsen, and Scharff.²⁰

The Thomas-Fermi screening radius a is

$$a = a_0 [0.885 / (Z_1^{2/3} + Z_2^{2/3})^{1/2}], \quad (\text{A5})$$

and

$$\epsilon = a/b \quad (\text{A6})$$

is the reduced energy (a dimensionless unit) introduced by Lindhard *et al.*²⁰ and b the collision diameter which can be calculated from

$$b = 2 \frac{Z_1 Z_2 e^2}{V^2} \left(\frac{m_1 + m_2}{m_1 m_2} \right), \quad (\text{A7})$$

where a_0 is the Bohr radius, and Z_1 , m_1 and Z_2 , m_2 are the atomic numbers and masses of incident ions of velocity V and the target atoms, respectively.

Two parameters, a reduced angle and thickness, $\tilde{\theta}$ and m , are introduced by Meyer and are defined by

$$\tilde{\theta} = \frac{1}{2} \epsilon [(m_1 + m_2)/m_2] \theta \quad (\text{A8})$$

and

$$m = \pi a^2 N t, \quad (\text{A9})$$

where θ is the total scattering angle and N and t are the atom density and thickness of the target, respectively.

The term $a^2 \pi N^{2/3} f_2(m, \tilde{\theta})$ in Eq. (A1) is usually only a small correction to $f_1(m, \tilde{\theta})$ and can be omitted.²¹ So

$$F(m, \tilde{\theta}) d\omega = \frac{1}{2\pi} d\omega \frac{\epsilon^2}{4} \left(\frac{m_1 + m_2}{m_2} \right)^2 f_1(m, \tilde{\theta}) \quad (\text{A10})$$

gives the distribution of particles being scattered into the solid angle $d\omega$ around the reduced scattering angle $\tilde{\theta}$.

By substituting Eq. (A8) in (A10) and noting that we are dealing with small-angle scattering,

$$F(m, \tilde{\theta}) d\omega = (1/2\pi) [f_1(m, \tilde{\theta}) 2\pi \tilde{\theta} d\tilde{\theta}]. \quad (\text{A11})$$

We now define a function $P(\tilde{\theta}_c)$ as the integrated normalized differential distribution of the particles scattered beyond angle $\tilde{\theta}_c$, namely,

$$P(\tilde{\theta}_c) = \int_{\tilde{\theta}_c}^\infty f_1(m, \tilde{\theta}) 2\pi \tilde{\theta} d\tilde{\theta} \quad (\text{A12})$$

and

$$P(0) = 1.$$

Application of the step-function approximation to the differential distribution of the particle in order to find the minimum yield assumes that a particle is in the random component of the beam (dechanneling probability equal to unity) when its angle with the channel axis is greater than $\tilde{\theta}_c$, the reduced critical angle for channeling, so we identify minimum yield χ_0 for a particular reduced film thickness m as

$$\chi_0 = P(\tilde{\theta}_c). \quad (\text{A13})$$

Determination of $\tilde{\theta}_c$. Substituting Eqs. (A6) and (A7) in (A8) yields

$$\tilde{\theta} = (aE/2Z_1 Z_2 e^2) \theta = Y(E, Z_1, Z_2) \theta, \quad (\text{A14})$$

where $E = \frac{1}{2} m V^2$ is the energy of incident ions and

$$Y(E, Z_1, Z_2) = aE/2Z_1 Z_2 e^2. \quad (\text{A15})$$

For crystals overlaid with metal films, the reduced critical angle $\tilde{\theta}_c$ is given by

$$\tilde{\theta}_c = Y(E, Z_1, Z_2) \psi_{1/2}, \quad (\text{A16})$$

where $\psi_{1/2}$ is the usual critical angle for channeling on uncovered crystals and $Y(E, Z_1, Z_2)$ is a normalizing factor.

*Work supported in part by the Office of Naval Research Grant No. N00014-69-A-0094-0022.

†Supported by African-American Institute Fellowship.

¹E. Bøgh and E. Uggerhøj, Nucl. Instr. Method **38**, 216 (1965).

²J. A. Davies, J. Denhartog, and J. L. Whitton, Phys. Rev. **165**, 345 (1968).

³E. Bøgh, Can. J. Phys. **46**, 653 (1968).

⁴S. T. Picraux, J. A. Davies, L. Eriksson, N. G. E. Johansson, and J. W. Mayer, Phys. Rev. **180**, 873 (1969).

⁵E. Rimini, E. Lugujo, and J. W. Mayer, Phys. Letters **37A**, 152 (1971).

⁶I. V. Mitchell, M. Kamoshida, and J. W. Mayer, J. App. Phys. **42**, 4378 (1971).

⁷E. Rimini, E. Lugujo, and J. W. Mayer, Phys. Rev. **B 6**, 716 (1972).

- ⁸J. F. Ziegler, *J. Appl. Phys.* **43**, 2973 (1972).
⁹S. T. Picraux, *Appl. Phys. Letters* **20**, 91 (1972).
¹⁰J. E. Westmoreland, J. W. Mayer, F. H. Eisen, and B. Welch, *Rad. Effects* **6**, 161 (1970).
¹¹S. T. Picraux, *J. Appl. Phys.* **44**, 587 (1973).
¹²H. H. Andersen, J. Böttiger, and H. Knudsen, *Rad. Effects* **13**, 203 (1972).
¹³L. Meyer, *Phys. Status Solidi* **44**, 253 (1971).
¹⁴G. W. Gobeli, *Phys. Rev.* **103**, 275 (1956).
¹⁵J. R. Comfort, J. F. Decker, E. T. Lynk, M. O. Scully, and A. R. Quinton, *Phys. Rev.* **150**, 249 (1966).
¹⁶D. I. Porat and K. Ramavataram, *Proc. Phys. Soc. (London)* **78**, 1135 (1961).
¹⁷O. Meyer, J. Gyulai, and J. W. Mayer, *Surface Sci.* **11**, 248 (1970).
¹⁸E. Kell, E. Zeitler, and W. Zinn, *Z. Naturforsch.* **15**, 1031 (1960).
¹⁹G. Molière, *Z. Naturforsch.* **3**, 78 (1948).
²⁰J. Lindhard, V. Nielsen, and M. Scharff, *Mat. Fys. Medd. Dan. Vid. Selsk.* **36**, 10 (1968).
²¹Peter Sigmund (private communication) points out that this term is an artifact from the specific approximation procedure used by Meyer.

Dynamical Properties of ⁵⁷Fe Dissolved in Al Observed by Mössbauer Effect

K. Sørensen and G. Trumpy

Laboratory of Applied Physics II, Technical University of Denmark, Lyngby, Denmark

(Received 29 August 1972)

The Mössbauer effect of ⁵⁷Fe in aluminum was measured over the temperature range 20–642 °C, using a source specimen of aluminum with ⁵⁷Co in solid solution. The line-broadening values were converted to diffusion constants, which can be expressed by the temperature dependence $D = 0.12 e^{-(1.4eV)/kT}$ cm²/sec. This result differs from recent diffusion-constant determinations obtained by the tracer-sectioning method, which we feel might be in error because of solution trapping. From theoretical considerations we suggest that a new expression for the correlation factor for the diffusional line broadening might be more accurate than the one used heretofore. Earlier determinations of the second-order Doppler shift were extended almost to the melting point of aluminum. The shift depends almost linearly on temperature, with the slope given by the Dulong–Petit rule for the heat capacity. From the temperature dependence of the Lamb–Mössbauer factor an effective Debye temperature of (210 ± 15) °K was found.

I. INTRODUCTION

The limit of solid solubility of iron in fcc metallic aluminum¹ is about 0.025 at.%. Because of this extremely small solubility, the solid-solution phase coexists with a clustered phase, except when the concentration is very small. The clustered state is of a complicated structure whose approximate composition² can be represented by Fe₄Al₁₃.

There is agreement between a number of experimental workers that the solid-solution phase, which undoubtedly is substitutional, gives a single unbroadened line in the Mössbauer spectrum, while the Fe₄Al₁₃ signal is a broad line with little structure. Bush, Stickels, and Hobbs³ investigated the effects of cold work and heat treatment on quenched samples. Janot and Lelay⁴ made similar studies of the effects of cold work on dilute alloys of iron in aluminum. Nasu and co-workers^{5,6} measured the shift of the solid-solution line as a function of temperature up to 450 °K, and from this they separated the thermal and the isomer shifts from each other. Preston and Gerlach⁷ used a specimen containing iron partly in the clustered state. They separated the overlapping signals

from the two phases by computer fitting and thus obtained data up to 675 °K, for both phases, on the line shift and Lamb–Mössbauer factor.

Bara and Hryniewicz⁸ prepared their source by first drying an aqueous solution of ⁵⁷CoCl₂ on an aluminum foil. After removal of the water of hydration by heating to 200–300 °C and then further heating in an argon atmosphere at 600 °C they obtained a complicated series of spectra which are not easily interpretable. The complexity was possibly due to the effects of oxidation, clustering, and trapping of the ⁵⁷Co atoms in the surface-oxide film.

In the present work the specimen was a very dilute ⁵⁷Co in aluminum source. With this specimen it was possible to extend the measurements up to near the melting point (660 °C) of aluminum, and thus obtain Mössbauer data on the solid-solution phase in the temperature range 20–642 °C. The real goal was, however, to study the diffusional broadening, which was observed from about 550 °C upwards. The study reported here appears to be the fourth study of diffusional broadening in solids. The first two by Knauer and Mullen were on diffusion of iron in copper⁹ and gold,¹⁰ while the